Anal Bioanal Chem (2002) 373 : 632–638
DOI 10.1007/s00216-002-1366-z

SPECIAL ISSUE PAPER

Sanford A. Asher · Serban F. Peteu · Chad E. Reese
Ming Xiang Lin · David Finegold

Polymerized crystalline colloidal array chemical-sensing materials for detection of lead in body fluids

Received: 6 December 2001 / Revised: 8 May 2002 / Accepted: 17 May 2002 / Published online: 11 July 2002

Abstract We have developed intelligent polymerized crystalline colloidal array (IPCCA) chemical-sensing materials for detection of Pb^{2+} in high ionic-strength environments such as body fluids with a detection limit of <500 nmol L^{-1} Pb^{2+} (100 ppb). This IPCCA lead sensor consists of a mesoscopically periodic array of colloidal particles polymerized into an acrylamide hydrogel. The array Bragg-diffracts light in the visible spectral region because of the periodic spacing of the colloidal particles. This material also contains a crown ether chelating agent for Pb^{2+}. Chelation of Pb^{2+} by the IPCCA in low-ionic-strength solutions results in a Donnan potential that swells the gel, which red-shifts the diffracted light in proportion to the Pb^{2+} concentration. At high ionic strength the Donnan potential is, unfortunately, swamped and no static response occurs for these sensors. We demonstrate, however, that we can determine Pb^{2+} at high ionic strength by incubating these IPCCA in a sample solution and then measuring their transient response on exposure to pure water. The non-complexed ions diffuse from the IPCCA faster than the bound Pb^{2+}. The resulting transient IPCCA diffraction red-shift is proportional to the concentration of Pb^{2+} in the sample. These IPCCA sensors can thus be used as sensing materials in optrodes to determine Pb^{2+} in high-ionic-strength solutions such as body fluids.

Keywords Intelligent polymerized crystalline colloidal array (IPCCA) · Pb^{2+} body fluid sensor · Photonic crystal · Bragg diffraction · Hydrogel chemical sensors

Dedicated to Professor David M. Hercules on the occasion of his 70th birthday

S.A. Asher (✉) · S.F. Peteu · C.E. Reese · M.X. Lin
Department of Chemistry, University of Pittsburgh, Pittsburgh, PA 15260, USA
e-mail: asher@pitt.edu

D. Finegold
School of Medicine, University of Pittsburgh, Pittsburgh, PA 15260, USA

Introduction

The development of novel clinical chemistry sensing methodologies is challenged technologically by the complexity of body fluids and by the relatively low concentrations of key analytes [1]. The acceptance of any new clinical chemistry methodology that fulfills the technological requirements is often limited by its cost and the requirement that the methodology be simple.

Our recent invention of intelligent polymerized crystalline colloidal array (IPCCA) chemical-sensing materials [2, 3, 4] might enable us to create new clinical chemistry methodologies that are able to fulfill the above requirements for a variety of different analytes. In the work described here we have demonstrated the applicability of IPCCA sensing materials to the detection of Pb^{2+} in body fluids. This work follows our previous demonstrations that IPCCA could be used to detect low concentrations of Pb^{2+} in low ionic-strength aqueous solutions [2, 3, 4].

Pb^{2+} is an important environmental toxin, which can cause disease and death at concentrations as low as 700 ppb in blood [5, 6]. Body concentrations as low as 100 ppb or 500 nmol L^{-1} might be correlated with reduced IQ in children. Universal screening of children for lead in blood was enunciated as a public health goal by the PHS and CDC in 1991. Current estimates from the national Center for Health Statistics state that 3.2% of American children have blood lead levels above 10 μg dL^{-1} (480 nmol L^{-1}). The rate for minority children in poverty is 20%.

Universal lead screening was abandoned by the federal government in 1997 for economic reasons, despite the large numbers of children at risk. Even when performed in large numbers the laboratory cost of analysis of a single blood specimen for lead is $8–15. The cost of drawing the blood, communicating the results, and, most importantly, finding and retrieving the child raise the price per case found to $50 or more. A rapid point of service method that would identify a child with an elevated lead level while the child is still present in the office would reduce the costs dramatically, and universal screening would once

again become a feasible goal. The impact of an inexpensive point of service quantitative serum lead test on prevention of serious lead poisoning and on the subsequent neurobehavioral casualty would be considerable.

United States (Center for Disease Control, CDC) and international (World Health Organization, WHO) guidelines both recommend that lead in body fluids should be measured with a detection limit of 10 μg dL^{-1} or 480 nmol L^{-1}, within a measuring range of 0–60 μg dL^{-1} or 0–2.88 μmol L^{-1} lead, and with a precision of less than 2 μg dL^{-1} or 10%, whichever is greater.

Several methods have been used to detect lead in biological matrices [1], including atomic absorption spectrometry, neutron activation analysis, spark-source mass spectroscopy, X-ray fluorescence, proton-induced X-ray emission, inductively coupled plasma atomic-emission spectroscopy, isotope dilution mass spectrometry, anodic stripping voltammetry (ASV), and differential pulse ASV. Reeder and Heineman [7] fabricated an electrochemical sensor by screen-printing techniques and coupled it with ASV to detect lead in the 10^{-6}–10^{-9} mol L^{-1} concentration range. An electrochemical analyzer coupled to screen-printed disposable sensors for field screening of trace lead was reported by Yarnitzky, Wang, and Tian [8] to detect 20–300 μg L^{-1} lead in drinking water. Yu et al. [9] made a lead sensor by first derivatizing Pb^{2+} with sodium tetraethylborate to form tetraethyllead which was then extracted from the headspace over the sample by solid-phase microextraction gas chromatography; the limit of detection was 5–10 ppb for urine and blood samples. Finally, de la Riva et al. [10] reported a flow-injection system which utilized room temperature phosphorescent quinolinesulfonic acid lead chelates immobilized on anion-exchange resin; this could be used to detect lead in seawater at the ng mL^{-1} level.

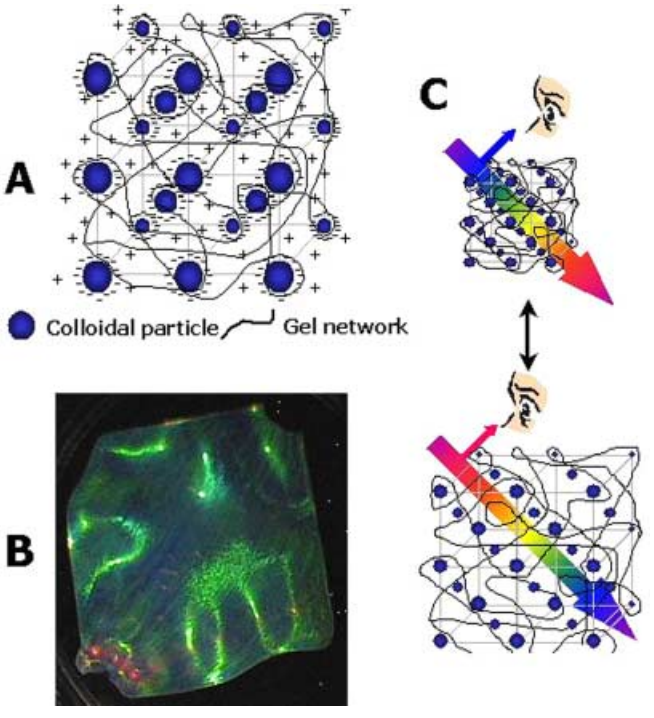

Fig. 1 **A**. Polymerized crystalline colloidal array showing a BCC array of polystyrene colloidal particles. Also shown schematically is the hydrogel polymer polymerized around the CCA. **B**. Photograph of IPCCA. **C**. Dependence of diffraction on IPCCA volume. As the IPCCA swells, the diffraction red-shifts

The IPCCA materials we are developing to detect Pb^{2+} in body fluids consist of a mesoscopically periodic array of colloidal particles [11, 12, 13, 14, 15, 16, 17, 18, 19, 20] polymerized into an acrylamide hydrogel [2, 3, 4, 21, 22, 23] (Fig. 1). This array diffracts light in the visible spectral region, because of the periodic spacing of the colloidal particles. The material also contains molecular recognition, or chelating, agents for the analytes of interest [2, 3, 4]. Because the IPCCA are >85% water, analyte species are free to rapidly diffuse into the IPCCA, with diffusion constants similar to those in water. These IPCCA are characterized by rich phase transition phenomena typical of hydrogels [24, 25, 26]. The Pb^{2+} sensing IPCCA contains a crown ether which selectively binds Pb^{2+} to the hydrogel.

The volume of the IPCCA hydrogel depends on three main factors – the free energy of mixing, the elastic free energy, and electrostatic interactions such as the formation of a Donnan potential, because of the presence of immobilized ions such as Pb^{2+} attached to the crown ether [27]:

$$\Delta G_{tot} = \Delta G_{mix} + \Delta G_{elas} + \Delta G_{elec} \quad (1)$$

The Donnan potential resulting from the bound Pb^{2+} results in an osmotic pressure which causes the gel to swell against the elastic gel restoring force [2, 3, 4] The resulting change in the particle array lattice constant shifts the diffracted wavelength [11, 12, 13, 14, 15, 16, 17, 18, 19, 20, 21, 22, 23] (Fig. 1C). Thus, the diffracted wavelength shift is indicative of the identity and concentration of the target analyte. We have already demonstrated that we can visually detect the presence of sub-ppm Pb^{2+}, and can instrumentally observe the diffraction shift from 20 ppb Pb^{2+}. We have also demonstrated that we could attach a small piece of this IPCCA to the end of an optical fiber and that the device obtained worked well [3, 4] as a sensitive optrode for the remote detection of Pb^{2+}.

The selectivity of this sensor depends on the selectivity of the crown ether molecular recognition group. Although K^+ could, potentially, interfere with our lead measurements, because it binds weakly to the crown ether, our results with fetal calf serum (discussed below) indicate that interference is insignificant.

In the work described here we further characterized and optimized IPCCA for detection of Pb^{2+}. As expected, these IPCCA sensors become less responsive to Pb^{2+} in high ionic strength aqueous solutions and become insensitive to Pb^{2+} at the ionic strengths of body fluids. We therefore developed a novel transient diffraction shift methodology that enables our IPCCA sensors to detect Pb^{2+} in body fluids.

Experimental

Chemicals and materials

Acrylamide (AMD), methylene bis-acrylamide (BIS), and lead nitrate were obtained from Fluka. 4-Acryloylamidobenzo-18-crown-6 (AAB18C6) and 2,2-diethoxyacetophenone (DEAP) were purchased from Acros Organics/Fisher Scientific, Pittsburgh, PA, USA. Sigmacote, an organopolysiloxane solution, was purchased from Sigma, St Louis, MO, USA. Fetal bovine serum (FBS) was purchased from GIBCO/Life Technologies, Grand Island, NY, USA. The FBS was delivered frozen and was thawed at room temperature, bottled as 25–100 mL aliquots, then re-frozen, and used as needed. Water was obtained from a Barnstead Nanopure water system.

IPCCA fabrication

We fabricated the Pb^{2+}-sensing IPCCA by using methods similar to those of Holtz et al. [2, 3, 4]. In the work described here, however, we used a Sigmacote hydrophobic coating on the quartz plates to aid release of the IPCCA after polymerization.

We utilized ~120-nm diameter highly charged, monodisperse polystyrene particles synthesized by means of a procedure reported elsewhere [28]. IPCCA samples were made with two different compositions. The composition of IPCCA A was close to that reported by Holtz [3] except that the concentration of the crown ether was doubled. A mixture of 103 mg AMD, 7.9 mg BIS, and 56 mg 4-acryloylamidobenzo-18-crown-6 in 160 mg water was added to 1.96 g of a 93 mg mL^{-1} dispersion of 120-nm colloidal particles. Ion-exchange resin (Bio-Rad, AG501-X8) and two drops of DEAP were added and the solution was gently shaken. The solution was centrifuged and the supernatant was injected into the chamber formed by two quartz cell flats separated by a 120-μm spacer. The cell was illuminated with UV light, after which it was opened to release the IPCCA film, which was washed overnight in water. IPCCA C incorporated additional crown ether (84 mg) and half the amount of cross-linker (3.95 mg).

We used a Spectral Instruments (Tucson, AZ, USA) model 400 CCD array spectrophotometer equipped with a bifurcated fiber-optic dip probe to determine the diffraction spectrum. A 9 around 1 fiber-optic probe immersed in the stirred solution illuminated the surface of the IPCCA attached to the quartz plate. Back-diffracted light was collected by the central fiber. The analyte and washing solutions were gently replaced between measurements.

Results and discussion

IPCCA Pb^{2+} in pure water

Figure 2 shows the dependence of the diffraction spectra of IPCCA A on Pb^{2+} concentrations between zero and 7.5 mmol L^{-1}. The diffraction peak red-shifts from 466 nm in pure water to 667 nm at 7.5 mmol L^{-1} Pb^{2+}. The red shift saturates at high Pb^{2+} concentrations, as previously observed by Holtz et al. [2, 3, 4]. This reduced IPCCA swelling response at high Pb^{2+} concentrations results from the increased solution ionic strengths that reduced the hydrogel swelling osmotic pressure (vide infra).

The topological plot of Fig. 3 A shows the dependence on time of the response of IPCCA C to changes in Pb^{2+} concentration. Spectra were measured every 10 s. When the IPCCA was immersed in pure water at t=0 the peak maximum was at 472 nm. At t=500 s the water was replaced with 75 μmol L^{-1} Pb^{2+} solution and the IPCCA

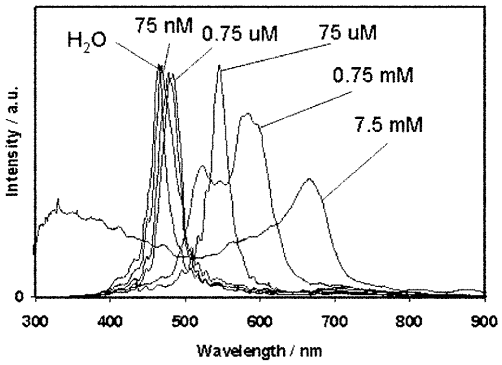

Fig. 2 Dependence on Pb^{2+} concentration of the IPCCA A diffraction spectrum in pure water. The diffraction from the 111 plane of the IPCCA crystal is measured in back-scattering mode. In the absence of Pb^{2+} we detect a sharp peak at 446 nm. The diffraction red-shifts as the Pb^{2+} concentration increases

swelled within 1 min and equilibrated within 8 min to red-shift the diffraction peak from 472 nm to 502 nm. At ~750 s, after the IPCCA ceased swelling, the Pb^{2+} solution was exchanged for pure water. The IPCCA diffraction then blue-shifted from 502 nm back to 472 nm. This blue shift was quasi-exponential with a time constant of ~3 min. At t=950 s the water was replaced with 750 μmol L^{-1} Pb^{2+} solution and the IPCCA diffraction red-shifted from 472 nm to 704 nm with a time constant of ~3 min. At ~1375 s the Pb^{2+} solution was replaced with pure water and the diffraction blue-shifted back to the original value with a time constant of ~2 min. Finally at ~2250 s, the water was replaced with 7.5 mmol L^{-1} Pb^{2+} solution and the IPCCA diffraction red-shifted from 472 nm to greater than 910 nm (the sensitivity of the CCD spectrometer is poor at these wavelengths). Replacement with pure water returned the diffraction back to 472 nm. These data demonstrate that the IPCCA response to Pb^{2+} is fully reversible even at relatively high Pb^{2+} concentrations.

Addition of 75 μmol L^{-1} Pb^{2+} results in almost rigid shifts of the narrow diffraction peaks, with little change in bandwidth. In contrast, larger changes in Pb^{2+} concentration can result in complex diffraction spectral changes. For example, Fig. 3B shows the diffraction spectra and the topological time dependence of the response to 750 μmol L^{-1} Pb^{2+}. The symmetric 472 nm peak at t=950 s shifts to ~670 nm, broadens and becomes asymmetric. This asymmetry presumably results from inhomogeneity in the Pb^{2+} concentration across the IPCCA, because of the short ~3 min diffusion time. A second transient red shift occurs on replacement of the 750 μmol L^{-1} Pb^{2+} solution with pure water. The 702 nm equilibrium peak maximum for 750 μmol L^{-1} Pb^{2+} (peak 4) transiently shifts to a 640 and 740 nm doublet (peak 5) upon water replacement. This doublet arises because although pure water exchanges with the bound Pb^{2+}, which will ultimately blue shift the IPCCA diffraction, the short time behavior results in a decrease in the ionic strength of the IPCCA solution which red-shifts the diffraction. We interpret the transient 740 nm peak as diffraction from an interior segment of the IPCCA that has a decreased ionic strength, whereas the 640 nm

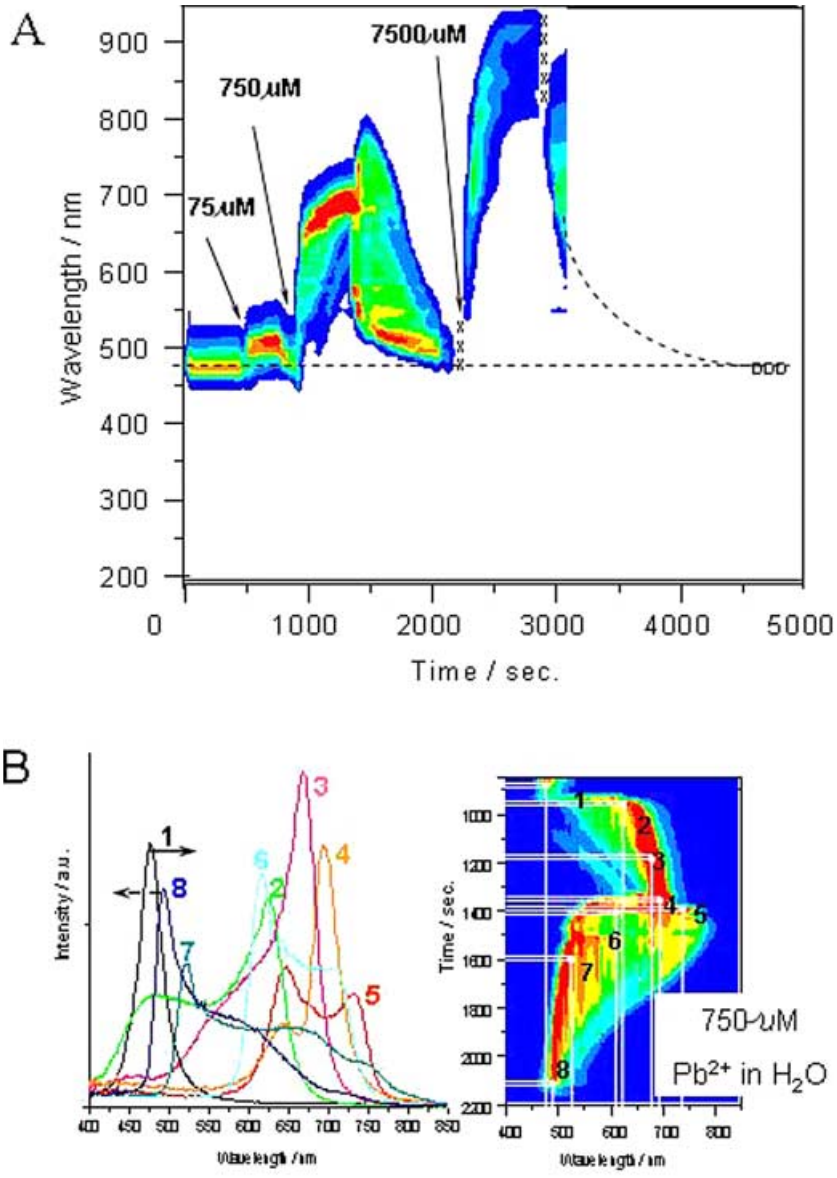

Fig. 3 **A**. Dependence on time of IPCCA C response to changes in Pb^{2+} concentration. Spectra were measured every 10 s. The IPCCA was immersed in pure water at t=0 and a maximum was observed at 472 nm. At t=500 s the water was replaced by 75 µmol L^{-1} Pb^{2+} solution. At ~750 s the Pb^{2+} solution was exchanged for pure water. At t=950 s the water was replaced with 750 µmol L^{-1} Pb^{2+} solution. At ~1375 s the Pb^{2+} solution was replaced with pure water. At ~2250 s the water was replaced with 7.5 mmol L^{-1} Pb^{2+} solution. Replacement with pure water returned the diffraction back to 472 nm. Areas denoted *XXX* were missed during data acquisition. The *dashed line* indicates the expected time course of the blue shift as the IPCCA relaxed in the pure water solution. At t=4500 s the diffraction occurs at the original value of 472 nm. **B**. Expanded plot of response of IPCCA C to 750 µmol L^{-1} Pb^{2+} (from Fig. 3A). Peak 4 shows essentially the equilibrium diffraction of the IPCCA in 750 µmol L^{-1} Pb^{2+} with a maximum at 704 nm. Replacement of the bathing solution with pure water results in a transient doublet, where the long wavelength component is red-shifted to 740 nm while the short wavelength component blue-shifts to 640 nm. The diffraction subsequently monotonically blue-shifts. See text for details

component results from an exterior segment where the Pb^{2+} concentration has decreased (vide infra, and see Fig. 4).

IPCCA Pb^{2+} response in 100 mmol L^{-1} NaCl

The response of the IPCCA to Pb^{2+} results from the formation of an osmotic pressure in the hydrogel because of immobilization of the Pb^{2+} cation within the crown ether. This forms an ionic gel. The immobilization of the Pb^{2+} counter-ion in low-ionic-strength solution causes a Donnan potential, which causes an osmotic pressure, which swells the gel. High-ionic-strength solutions attenuate the Donnan potential and reduce the swelling and, thus, decrease the sensitivity of the IPCCA to Pb^{2+}. Thus the sensitivity of our IPCCA Pb^{2+} sensor and our glucose sensor are poor when used directly in body fluids, which are >150 mmol L^{-1} in salt.

There is, however, a fractionating chemical sensing principle that could be devised to make these IPCCA sensors detect Pb^{2+} in high-ionic-strength solutions. Figure 4 shows the detection scheme. Incubation of the IPCCA sensor in 100 mmol L^{-1} NaCl solution containing Pb^{2+} results in binding of the Pb^{2+} to the crown ether (Na^{+} might compete somewhat for crown ether binding, because of its high concentration). Little IPCCA diffraction shift is expected in this high-ionic-strength solution compared with that in pure water, because little osmotic pressure is induced by Pb^{2+} binding. After equilibration with the high-ionic-strength analyte solution, the IPCCA is placed in pure water. The IPCCA is mainly water (>85%) and the ions diffuse out, with diffusion constants similar to those in pure water. As the ionic strength decreases the IPCCA gel swells in proportion to the amount of cations bound. As time progresses the Pb^{2+}, which is bound most strongly, is retarded and transient IPCCA swelling occurs and a

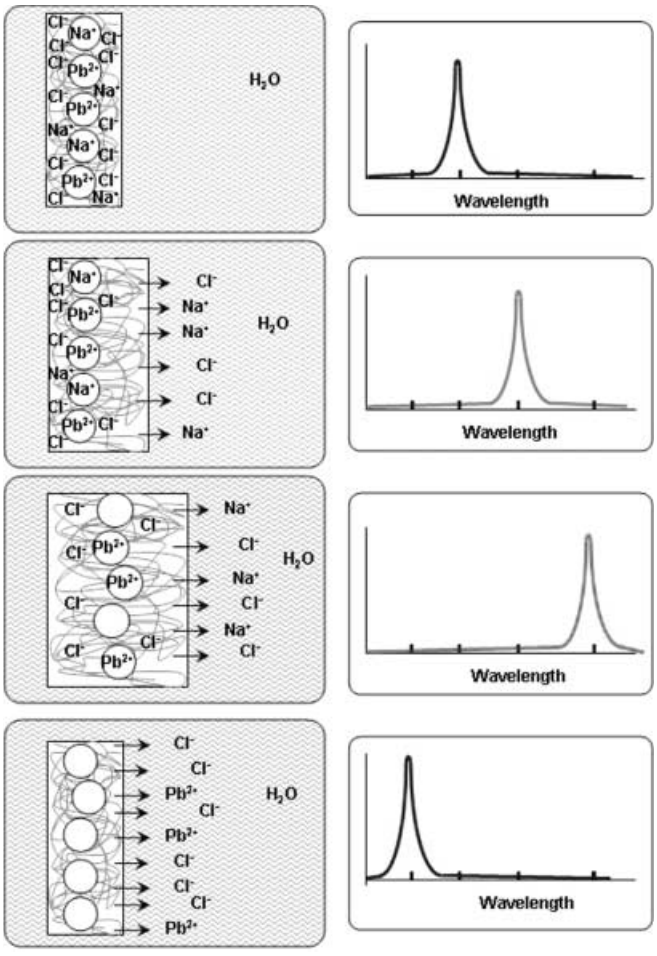

Fig. 4 Mechanism of IPCCA transient response to exposure to pure water. At high salt concentrations the response of the IPCCA to Pb^{2+} binding to the crown ether is poor, because of the high ionic strength of the IPCCA solution. Exposure to pure water causes diffusion of NaCl out of the gel. The diffusion of the crown ether-bound Pb^{2+} is delayed. Thus, a transient diffraction red shift occurs as the IPCCA solution ionic strength decreases

transient diffraction red shift occurs. This transient red shift is followed by a diffraction blue shift as the Pb^{2+} finally diffuses out of the IPCCA.

As shown below, we have utilized this transient response methodology to enable IPCCA measurements of Pb^{2+} in high-ionic-strength solutions and in body fluids. We are also developing quantitative diffusion models for this sensing principle; this will be presented elsewhere.

The IPCCA responds little to NaCl in solution. For example, IPCCA C in pure water diffracts 476 nm light. Immersion in 100 mmol L^{-1} NaCl solution results in a transient blue shift, because of the osmotic pressure associated with the NaCl concentration difference between the interior of the IPCCA and the bathing NaCl solution. After 10 min, however, the NaCl concentrations equilibrate and we observe a net 9-nm red shift. This red shift presumably results from an increase in the free energy of mixing of the hydrogel, because of binding of Na^+ to the crown ether. Replacement of the NaCl solution with pure

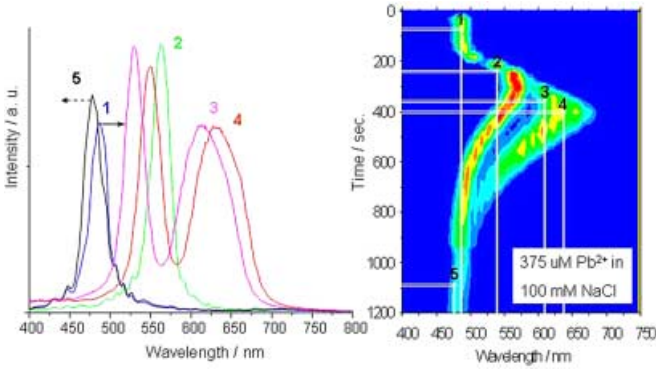

Fig. 5 Transient response of IPCCA C in 375 μmol L^{-1} Pb^{2+} in 100 mmol L^{-1} NaCl to pure water. The IPCCA initially diffracts 489 nm light. The maximum red-shifted diffraction appears as a doublet of a 548 nm almost symmetric peak and a 630 nm broad, skewed peak (peak 4)

water blue-shifts the diffraction back to 476 nm. We see no transient red shift upon exchanging the 100 mmol L^{-1} NaCl with pure water, presumably because of the low affinity and the fast rate of removal of the Na^+ from the crown ether.

Although no diffraction change is observed upon addition of Pb^{2+} to the IPCCA in 100 mmol L^{-1} NaCl, Fig. 5 demonstrates the large transient red shift which occurs for IPCCA C incubated with 375 μmol L^{-1} Pb^{2+}, 100 mmol L^{-1} NaCl solution upon exchange with pure water. The diffraction wavelength initially occurs at 489 nm in the Pb^{2+}-NaCl solution. Upon exchange with pure water, we see a large transient red shift for this high concentration Pb^{2+} solution. The maximum red-shifted diffraction appears as a doublet consisting of a 548 nm almost symmetric peak and a 630 nm broad, skewed peak (Fig. 5, peak 4). This doublet is presumably because of ionic strength and Pb^{2+} concentration inhomogeneity across the IPCCA thickness. As expected, the magnitude of the transient response increases monotonically as the Pb^{2+} concentration increases. We are currently modeling diffusion of Pb^{2+} and NaCl out of the IPCCA to understand this phenomenon in detail.

These results indicate that we can use this transient IPCCA response to detect Pb^{2+} in high-ionic-strength solutions such as body fluids. Further, the magnitude of the response increases as the Pb^{2+} concentration increases. The studies below examine this transient response to Pb^{2+} in a model body fluid, bovine calf serum.

Measurements of Pb^{2+} in fetal bovine serum

We examined the response of our IPCCA C to Pb^{2+} in fetal bovine serum (FBS), in which salt concentrations are similar to those found in blood (140 mmol L^{-1} Na^+, for example). We prepared the highest concentration FBS stock solution by dissolving a weighed amount of lead nitrate in a large volume of FBS. FBS solutions containing lower concentrations of lead nitrate were obtained by mixing the stock solutions with pure FBS.

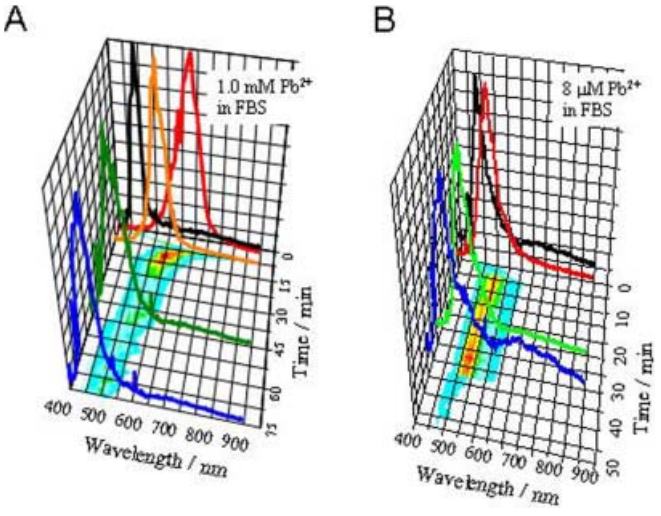

Fig. 6 **A**. 3D diffraction plot of the response of IPCCA C incubated in pure FBS, then exposed to a solution of 1.0 mmol L^{-1} Pb^{2+} in FBS, and finally exposed to pure water. The IPCCA diffracted at 481 nm in pure FBS and in the 1.0 mmol L^{-1} Pb^{2+} FBS solution. Exchange of the 1.0 mmol L^{-1} Pb^{2+} FBS solution for pure water results in a transient red shift to a 680 nm maximum within 5 min. A blue shift to 550 nm occurs by 8 min and to 483 nm by 60 min. **B**. 3D diffraction plot of the transient response of IPCCA C incubated in 8 µmol L^{-1} Pb^{2+} FBS solution. The IPCCA initially diffracted at 480 nm in 8 µmol L^{-1} Pb^{2+} and transiently red-shifted to a maximum of 532 nm within 5 min. By 40 min, the diffraction peak blue-shifted back to ~480 nm

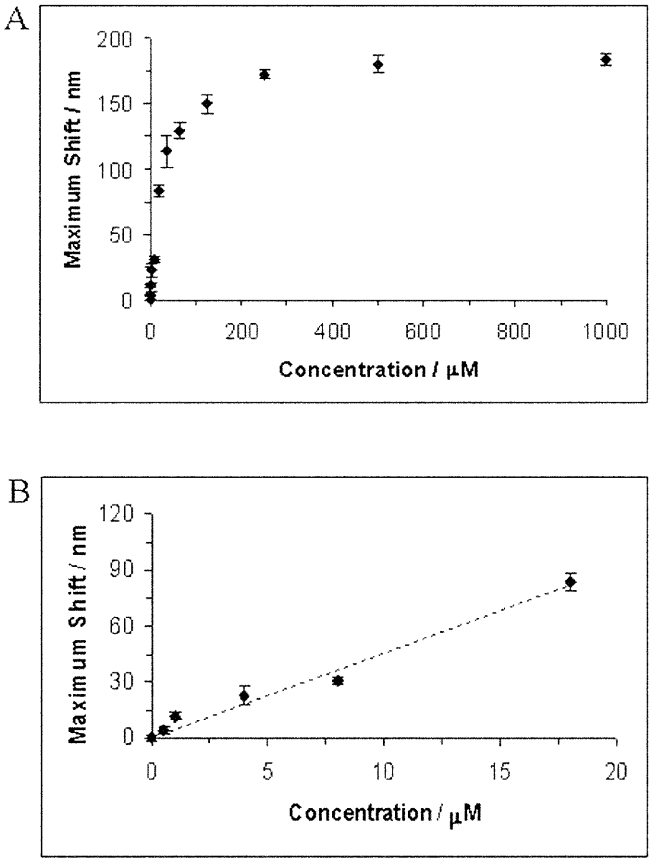

Fig. 7 **A**. Dependence on Pb^{2+} concentration in FBS of the maximum diffraction wavelength-shift observed for IPCCA C. **B**. Expanded plot of the dependence of the maximum diffraction wavelength shift observed for IPCCA C on Pb^{2+} concentrations in FBS between 0 and 20 µmol L^{-1} Pb^{2+}. The detection limit is <0.5 µmol L^{-1} Pb^{2+}. The best-fit line is shown

We are aware that Pb^{2+} binds to proteins and other species present in body fluids and this binding should reduced the availability of Pb^{2+} to the IPCCA [1, 5, 6]. If, however, Pb^{2+} can exchange between sites, the Pb^{2+} concentration detected will depend upon the relative affinity of the crown ether for Pb^{2+} compared with other FBS chelating species.

The response of the IPCCA to the FBS solution was similar to that observed for the NaCl solution. For example, a 20 nm red shift is observed for IPCCA C on transfer from pure water to FBS, followed by a slow blue shift (1 h) back to its original pure water diffraction wavelength.

Figure 6A shows the transient response of IPCCA C which was first incubated in pure FBS, then exposed to a solution of 1.0 mmol L^{-1} Pb^{2+} in FBS, and then exposed to pure water. The IPCCA diffracted at 481 nm in pure FBS in the absence of Pb^{2+}. When the FBS solution was exchanged for 1.0 mmol L^{-1} Pb^{2+} FBS solution no significant shift was observed in the diffraction wavelength, indicating that the high FBS ionic strength swamps the IPCCA response to Pb^{2+}. Exchange of the 1.0 mmol L^{-1} Pb^{2+} FBS solution for pure water resulted in a large transient red shift, the 680 nm maximum of which occurred in 5 min. The gel blue-shifted back to 550 nm within 8 min and to 483 nm in 60 min. Obviously the transient response time of the IPCCA is slower in FBS than in 100 mmol L^{-1} NaCl.

Figure 6B shows measurement of a lower concentration of 8 µmol L^{-1} Pb^{2+} in FBS solution. The IPCCA initially diffracted at 480 nm in both the pure FBS and in the 8 µmol L^{-1} Pb^{2+} FBS solution. On exposure to water the IPCCA transiently red shifted to a maximum value of 532 nm within 5 min. After 40 min, the IPCCA blue-shifted to its value in pure water of ~480 nm.

The maximum transient diffraction red shift in FBS associated with Pb^{2+} binding is plotted in Fig. 7A. Figure 7B shows the linear portion of Fig. 7A. These maximum transient shifts are those above the 20 nm red shift of the IPCCA due to pure FBS. For example, the 4 nm response reported here for 0.5 µmol L^{-1} Pb^{2+} was actually a 24 nm total red shift. The IPCCA response to Pb^{2+} in FBS saturates at concentrations above ~100 µmol L^{-1} Pb^{2+}, where the crown ether binding sites become saturated. Because the standard deviation in the detected wavelength shift is ~1 nm, this indicates a detection limit of less than 500 nmol L^{-1} Pb^{2+}.

This detection limit is similar to the 0.48 µmol L^{-1} Pb^{2+} detection limit recommended by the United States Center for Disease Control (CDC) and the World Health Organization (WHO) for sensing lead in whole blood. We are now beginning studies of hemolyzed whole blood and of urine (lead concentration ~3–4 fold that of whole blood)

to determine the lead detection limits in these body fluids. Lead concentrations in urine correlate linearly with whole blood lead levels [29, 30].

Unfortunately, our detection limit is too large for use in the detection of lead in serum, because lead concentrations are a factor of thirty less than in whole blood [29, 30, 31, 32, 33, 34]. We have not yet optimized these Pb^{2+} IPCCA sensors. It is likely we can dramatically increase their sensitivity such that they can be used to detect lead in serum. We can increase IPCCA sensitivity by reducing its cross-link density, increasing the concentration of crown ether, and by increasing the crown ether binding affinity. Reducing the cross-linker concentration reduces the hydrogel elastic constant which makes the IPCCA more responsive. Increasing the concentration of crown ether and increasing its binding affinity increases the number of lead cations bound at low lead concentrations, which makes the sensor more sensitive.

Conclusions

We have demonstrated the applicability of IPCCA sensors for the detection of Pb^{2+} in body fluids and high-ionic-strength environments. These sensors utilize a change in the diffraction wavelength from a crystalline colloidal array imbedded in a hydrogel which has attached crown ether groups. These crown ether groups chelate Pb^{2+} with a high degree of specificity and sensitivity. We use a transient response method to detect Pb^{2+} binding in these high-ionic-strength environments because the ionic interferents in this matrix swamp the Donnan potential associated with Pb^{2+} binding.

Our transient response method consists of incubating the IPCCA with the solution to be tested followed by washing the hydrogel with pure water. When the unbound ions are washed out the remaining bound ions give rise to a Donnan potential which results in an osmotic pressure which swells the hydrogel and red-shifts the diffraction. The magnitude of the diffraction wavelength-shift depends on the Pb^{2+} concentration. We observed a detection limit of $<0.5\ \mu mol\ L^{-1}\ Pb^{2+}$.

Because these IPCCA Pb^{2+} sensors should be inexpensive to manufacture and are reusable, they should be able to find applications in areas such as water testing and measuring lead in blood. For applications at higher Pb^{2+} ($\sim 10\ \mu mol\ L^{-1}$) concentrations the IPCCA response is visible to the human eye, whereas lower concentrations will require the use of a small, inexpensive spectrophotometer for detection. This sensor can obviously be easily modified for detection of other ionic analytes by changing the chelating molecular recognition agent.

Acknowledgements We gratefully acknowledge support for this work from NIH grant 1-R01 GM 58821-01, ONR grant N00014-94-0592, and DOE grant DE-FG07-9BER62708.

References

1. Burtis CA, Ashwood ER (1999) (eds) Tietz textbook of clinical chemistry. Saunders, Philadelphia
2. Holtz JH, Asher SA (1997) Nature 389:829–832
3. Holtz JH, Holtz JSW, Munro CH, Asher SA (1998) Anal Chem 70:780–791
4. Asher SA, Holtz JH, (1998) US Patent 5854078 and (1999) US Patent 5898004
5. Royce SE, Needleman HL (1990) (eds) Case studies in environmental medicine lead toxicity. US Public Health Services ATSD
6. Adam DA, Buss-Frank MJ (1995) Pediatric Nursing 10:194–198
7. Reeder GS, Heineman WR (1998) Sens Actuators B 52:58–64
8. Yarnitzky C, Wang J, Tian B (2000) Talanta 51:333–338
9. Yu X, Yuan H, Gorecki T, Pawliszyn J (1999) Anal Chem 71: 2998–3002
10. De la Riva BSV, Costa-Fernandez JM, Pereiro R, Sanz-Medel A (1999) Anal Chim Acta 395:1–9
11. Asher SA, Flaugh PL, Washinger G (1986) Spectroscopy 1:26–31
12. Rundquist PA, Photinos P, Jagannathan S, Asher SA (1989) J Chem Phys 91:4932–4941
13. Kesavamoorthy R, Super MS, Asher SA (1992) J Appl Phys 71:1116–1123
14. Asher SA, Kesavamoorthy R, Jagannathan S, Rundquist P (1992) SPIE 1626:238–241
15. Asher SA, Holtz J, Liu L, Wu Z (1994) J Am Chem Soc 116: 4997–4998
16. Tse A, Wu Z, Asher SA (1995) Macromolecules 28:6533–6538
17. Asher SA, Tse A, Liu L, Pan G, Wu Z, Li P (1995) Mat Res Soc Symp Proc 374:305–310
18. Asher SA, Pan G (1996) In: Fendler JH (ed) Nanoparticles in solids and solutions, NATO ASI Series Vol 18. Kluwer Academic Publishers, Dordrecht 65–69
19. Liu L, Li P, Asher SA (1997) J Am Chem Soc 119:2729–2732
20. Pan G, Kesavamoorthy R, Asher SA (1997) Phys Rev Lett 78: 3860–3863
21. Weissman JM, Sunkara HB, Tse AS, Asher SA (1996) Science 274:959–960
22. Kesavamoorthy R, Pan G, Asher SA (1997) In: Kesavamoorthy R, Rao CB, Arora AK, Kalyanasundaram P (eds) Laser applications in material science and industry. Allied, New Delhi, pp 265–273
23. Sunkara HB, Weissman JM, Penn BG, Frazier DO, Asher SA (1996) Polym Prepr 37:453–454
24. Dusek K (1993) (ed) Responsive gels: volume phase transitions, Advances in polymer science 109. Springer, Berlin
25. Dusek K (1993) (ed) Responsive gels: volume phase transitions II, Advances in polymer science 110. Springer, Berlin
26. Okano T (1993) Adv Polym Sci 110:179–197
27. Flory J (1953) Principles of polymer science. Cornell University Press, Ithaca
28. Reese CE, Guerrero CD, Weissman JM, Lee K, Asher SA (2000) J Colloid Interface Sci 232:76–80
29. Cavalleri A, Minoia C, Pozzoli L, Baruffini A (1978) Br J Ind Med 35:21–26
30. Manton WI, Cook JD (1984) Br J Ind Med 41:313–319
31. Everson J, Patterson CC (1980) Clin Chem 26:1603–1607
32. DeSilva PE (1981) Br J Ind Med 38:209–217
33. Marcus AH (1985) Environ Res 36:473–489
34. Cake KM, Bowins RJ, Vaillancourt C, Gotdon CL, McNutt RH, Laporte R, Webber CE, Chettle DR (1996) Am J Ind Med 29:440–445